Local-S shear wave splitting along the length of the Alaska-Aleutian subduction zone

Colton Lynner[1*], Cherilyn Toro-Acosta[2], Eve Paulson[3], and Andrew Birkey[1]

[1]Department of Earth Sciences, University of Delaware, [2]Department of Geology, University of Puerto Rico at Mayagüez, [3]Department of Geology, Pomona College
*corresponding author: clynner@udel.edu

Keywords: Seismic anisotropy; Subduction zone processes; Mantle processes

Abstract

The Alaska-Aleutian subduction zone represents an ideal location to study dynamics within a mantle wedge. The subduction system spans several thousand kilometers, is characterized by a slab edge, and has ample seismicity. Additionally, the majority of islands along the arc house broadband seismic instruments. We examine shear wave splitting of local-S phases originating along the length of the subduction zone. We have dense measurement spacing in two regions, the central Aleutians and beneath Alaska. Beneath Alaska, we observe a rotation in fast splitting directions near the edge of the subducting slab. Fast directions change from roughly trench perpendicular away from the slab edge to trench parallel near the boundary. This is indicative of toroidal flow around the edge of the subducting Alaska slab. In the central Aleutians, local-S splitting is primarily oriented parallel to, or oblique to, the strike of the trench. The local-S measurements, however, exhibit a depth dependence where deeper events show more consistently trench parallel directions indicating prevalent trench parallel mantle flow. Our local-S shear wave splitting results suggest trench parallel orientation are likely present along much of the subduction zone excited by the slab edge, but that additional complexities exist along strike.

1. Introduction

The Alaska-Aleutians subduction zone (AASZ) spans ~3500 kilometers and includes along strike variations in several subduction parameters, such as changes in slab dip [Lallemand et al., 2005], plate age [Heuret and Lallemand, 2005], plate motion [DeMets et al., 2010], paleo-spreading direction [Maus et al., 2009], and earthquake behavior [Davies et al., 1981; Fournier and Freymueller, 2007; Shillington et al., 2015]. Most notably, the AASZ is characterized by the edge of the subducting Pacific Plate located beneath Alaska [Eberhart-Phillips et al., 2006; Ferris et al., 2003; Martin-Short et al., 2018]. Several studies have examined the dynamics associated with such a slab edge and have suggested they excite more complex patterns of flow within the subduction system [e.g. Honda, 2009; Jadamec and Billen, 2010, 2012; Kincaid and Griffiths, 2003; Piromallo et al., 2006; Stegman et al., 2006]. In most cases, a free slab edge excites toroidal flow around the structure leading to trench parallel mantle flow [Jadamec and Billen, 2010, 2012; Piromallo et al., 2006; Stegman et al., 2006]. Toroidal flow has been suggested in many subduction settings globally to account for trench parallel observations of anisotropy [e.g. Civello and Margheriti, 2004; Peyton et al., 2001; Song et al., 2021] including in the AASZ [Christensen and Abers, 2010; Hanna and Long, 2012; McPherson et al., 2020; Venereau et al., 2019; Yang et al., 2021].

Observations of seismic anisotropy can offer direct evidence of deformation and flow within the mantle wedge [e.g. see reviews by Savage, 1999 and Long and Silver, 2009]. As the mantle deforms, olivine grains tend to rotate relative to the orientation of maximum extensional strain, acting as a proxy for the direction of flow [e.g. Karato et al., 2008]. Shear wave splitting is one of the most direct measurements of the orientation and strength of anisotropy [see review by Long and Silver, 2009]. The relationship between shear wave splitting orientations and the direction of strain is dependent upon mantle stress conditions and water content [e.g. Karato et al., 2008]. For the majority of the upper mantle, stress conditions and water contents are low enough such that olivine A-, C-, and/or E-type fabrics develop. Each of these fabric types are characterized by fast splitting directions that parallel strain [e.g. Karato et al., 2008; Lynner et al., 2017]. In high stress, high water content regions, however, olivine B-type fabric can arise [Jung et al., 2006]. B-type fabric produces the opposite splitting relationship to strain, where fast splitting directions orient perpendicular to strain. In the corner of the mantle wedge, stresses and water contents can be high enough to produce B-type fabrics [e.g. Kneller et al., 2008; McCormack et al., 2013]. Elsewhere in the mantle wedge, A-, C-, or E-type fabrics likely dominate [Karato et al., 2008], which can make interpreting shear wave splitting in subduction zones challenging.

Shear wave splitting of S phases arising from local earthquakes within a subduction zone (referred to as local-S splitting) offers an excellent means of probing anisotropy within the mantle wedge. Local-S splitting has been employed in a number of subduction zones worldwide [e.g. Liu et al., 2008; Hammond et al., 2010; Kong et al., 2020], including in Alaska [Karlowska et al., 2021; Richards et al., 2021; Yang et al., 1995; Yang et al., 2021], to great success. Since it uses local earthquakes rather than distant teleseismic events, local-S splitting allowing us to place constraints on the depth of anisotropy. Any observed shear wave splitting must originate due to anisotropy between the event and the surface, avoiding potential complications like subslab anisotropy [Lynner and Long, 2014]. Local-S splitting is often interpreted only in terms of anisotropy in the mantle wedge despite anisotropy potentially being present in the upper plate and in the downgoing slab [e.g. Wirth and Long, 2010; Karlowska et al., 2021; Richards et al., 2021]. Contributions to local-S splitting from slab anisotropy are generally negligible due to the minimal amounts of slab material sampled by the local-S phases. The upper plate may host some anisotropy, but previous studies have shown that crustal splitting tends to be very small (between 0.1s and 0.3s) [Kaneshima, 1990; Crampin and Peacock, 2008]. Additionally, recent studies have shown that the forearc mantle of the upper plate may be largely isotropic [e.g. Uchida et al., 2020]. Therefore, local-S splitting primarily originates due to anisotropy within the mantle wedge.

While the Alaskan region has been the focus of many studies [e.g. Christensen and Abers, 2010; Hanna and Long, 2012; Debayle et al., 2016; Karlowska et al., 2021; Lynner, 2021; McPherson et al., 2020; Perttu et al., 2014; Richards et al., 2021; Venereau et al., 2019; Yang et al., 1995; 2021], a detailed picture of how wedge anisotropy varies along the length of the AASZ has been lacking due to poor seismic coverage along the Aleutian arc. This changed in 2019 when many broadband seismic stations along the length of the subduction zone were serviced and brought back into operation. There are now nearly 200 broadband stations operating along the length of the AASZ. Abundant slab seismicity and dense station coverage (Fig. 1) allows for a high resolution look at wedge anisotropy along the length of the subduction zone. In this study, we examine local-S shear wave splitting at all the broadband seismic stations operating along the length of the Alaska-Aleutian subduction zone.

2. Methods

We measure shear wave splitting of local-S phases at all broadband seismic stations operating along the length of the Alaska-Aleutian subduction zone from the beginning of data availability at each station until June 2022. The majority of seismic stations have data for ~3 years between 2019 and 2022. A few long-running stations have more than 20 years of data. We restrict measurements to local events greater than magnitude 4.5. Local events are defined as those originating in the subducting slab beneath a station such that the incoming direct S phase has a vertical incidence angle of less than 35º. This has been shown to produce reliable local-S splitting results [e.g. Wirth and Long, 2010]. We further restrict our analysis to earthquakes located deeper than 75 km to ensure adequate wedge material is being sampled. The deepest events in our dataset are shallower than ~250 km.

We use the SplitLab software package [Wüstefeld et al., 2008] to perform shear wave splitting measurements. All seismograms are bandpass filtered between 8 and 25 seconds [e.g. Long and van der Hilst, 2006; Lynner et al., 2022]. We visually inspect each waveform for the clear arrival of the direct S wave. We employ the simultaneous use of the Rotation Correlation [e.g. Bowman and Ando, 1987] and eigenvalue minimization [e.g. Silver and Chan, 1991] methods to measure fast directions and delay times. Unlike traditional XKS splitting studies, local-S phases do not have known initial polarizations, which is why we use the eigenvalue minimization method [e.g. Wirth and Long, 2010]. Results are reported using the Rotation Correlation method, but we require that the agreement between both methods is within 15º for fast direction and 0.5 s for delay time. All shear wave splitting results retained in this study have individual errors in fast direction of less than 30º and less than 0.9 s for delay time. On average, errors in fast direction are ~14.8º and errors in delay time are ~0.3s. Null observations are based on the linearity of the uncorrected particle motion [Wüstefeld and Bokelmann, 2007].

3. Results

We examined local-S shear wave splitting at 193 broadband stations along the length of the subduction zone (Table S1). Many stations yielded no splitting observations, and the majority provided fewer than two measurements that met our quality control criteria (Fig. 1). This is largely due to noise issues arising from extreme proximity to coastal noise sources. In total, we made 114 split measurements and 204 null observations (Figs. 2, S1, and S2, Table S1). The majority of our observations fall into two geographic locations: 1) the eastern the portion of the subduction system beneath Alaska and 2) the central portion of the Aleutian arc between ~175ºE and ~160ºW.

In the central Aleutians, splitting directions are broadly oriented parallel to, or oblique to, the strike of the trench. The trench oblique fast directions are aligned nicely with the motion of the downgoing Pacific Plate [DeMets et al., 2010]. The eastern portion of our study area beneath Alaska contains the bulk of our shear wave splitting measurements (Figs. 2 and S3). In this region, fast directions rotate from strongly trench perpendicular in the south to strongly trench parallel in the north over the span of ~400 km. This pattern is robust as it is driven by observations at multiple stations along the length of the subduction zone. Additionally, nearby observations are self-consistent suggesting a robust anisotropic feature. Delay times are less varied throughout this region with an average delay time of ~0.9s.

We have great confidence in our local-S splitting observations in the regions of dense measurements. The agreement seen regionally between nearby measurements suggests the anisotropic features being imaged are prominent. We also document several instances where single events yielded consistent splitting results at multiple stations (Fig. S4). These examples show that individual measurements are not being heavily biased by differences in shallow crustal anisotropy and instead reflect anisotropy throughout the wedge.

4. Discussion

4.1 Mantle wedge splitting beneath Alaska

We observe local-S shear wave splitting along much of the length of the AASZ (Fig. 2). We see areas of trench parallel as well as plate-motion parallel splitting suggesting complex anisotropy within the mantle wedge consistent with previous studies [e.g. Karlowska et al., 2021; Long and Silver, 2008; Richards et al., 2021]. The best lateral density of local-S shear wave splitting measurements is found in the eastern portion of our study region beneath Alaska (Fig. 2). Splitting recovery in this area is greatly improved by the EarthScope Transportable Array stations [IRIS Transportable Array, 2003] and by larger landmasses.

Beneath Alaska, we observe a distinct transition in fast splitting directions from plate motion parallel in the south to trench parallel in the north. This transition happens gradually over ~400km and is marked by fast directions that sweep through intermediate orientations. Our results are broadly similar to previous local-S shear wave splitting studies, where trench-parallel fast directions were seen in the Central Aleutians [Yang et al., 1995] and in the forearc beneath Alaska [Karlowska et al., 2021; Richards et al., 2021]. In the backarc, fast directions rotate to trench-oblique or perpendicular [Karlowska et al., 2021; Richards et al., 2021], which mirrors our findings in southern Alaska.

The transition in fast directions beneath Alaska is likely related to the edge of the subducting Alaskan slab. Yang et al. (2021) observe similar complexity in fast directions to the northeast of our study area, which they also attribute to toroidal flow around the slab edge. Such a change in fast directions is predicted by geodynamic models that show slab edges can excite toroidal flow [Jadamec and Billen, 2010; 2012; Schellart and Moresi, 2013; Király et al., 2017]. The Alaskan slab terminates just east (within ~500 km) of the transition to trench parallel splitting seen in our dataset. Toroidal return flow around the edge of the slab would yield trench parallel fast directions in the mantle wedge that transition to normal entrainment of mantle wedge material. This is consistent with our observations where splitting measurements further south exhibit plate motion aligned fast directions. The transition in fast directions happens quickly over a lateral distance of roughly 400 km. This is a smaller length scale than is predicted by geodynamic models [e.g. Jadamec and Billen, 2010; 2012] suggesting the toroidal flow may be stronger than previously proposed. This observation will prove useful in refining future numeric models aimed at understanding mantle dynamics around the edge of this subducting Alaskan slab.

There is the potential for B-type olivine fabric in the corner of the mantle wedge beneath Alaska where stresses are high [Jung et al., 2006]. Should a transition in olivine fabric exist, there would be a noticeable change in anisotropy [e.g. McCormack et al., 2013] due to the antithetic relationship between splitting and strain exhibited by B-type fabric. Regions where B-type olivine has been suggested exhibit event depth dependent shear wave splitting where shallow events near the trench show nearly orthogonal fast directions to results from deeper events [e.g. Long and van der Hilst, 2006]. We see no such relationship between fast directions and event depth, Fig. 3. Deep (>200 km) events show the same pattern in splitting as the shallow events. Additionally, the predicted change in splitting directions due to a fabric type change is abrupt and nearly orthogonal. We see a gradual change in fast direction that sweeps through intermediate orientations. The lacking correlation between fast directions and depth and the gradual change in splitting suggests consistent olivine fabrics are being sampled by the local-S phases. Previous local-S splitting studies, however, have yielded conflicting interpretations of the role of B-type olivine beneath Alaska. Karlowska et al. [2021] also argue against the presence of

B-type fabric in the mantle wedge beneath Alaska based on the continuity of splitting results throughout the region. Richards et al. [2021], however, suggest B-type olivine as one possible explanation for their splitting results. Our results suggest there is likely no impact on splitting from B-type fabric in the Alaska region.

4.2 Splitting from the wedge in the central Aleutians

In the central Aleutians, splitting measurements are either parallel to, or highly oblique to, the strike of the trench. The variability in fast directions, however, disappears when examining only deep earthquakes, Fig. 3. Deeper earthquakes yield more consistently trench parallel fast directions than shallower events. Depth dependent fast directions can be tied to sampling of larger volumes of mantle wedge material and/or changes in anisotropic fabrics. Stronger flow orientations can develop in the thicker regions of the wedge that deeper events sample. Deep event S-waves also traverse farther from the corner of the wedge where olivine B-type fabric could exist. The shallowest events in our dataset (~75km depth) may be sampling less than ~50 km of mantle wedge material, are very near the corner, and correspondingly exhibit complex splitting behavior.

The dominant splitting direction in the central Aleutians is trench parallel. This type of splitting is found at all depths and comprises the majority of observations in the region. Further, deep measurements show more consistently trench parallel orientations suggesting splitting is driven by dynamics and not due to B-type olivine fabric. We interpret the trench parallel splitting as the primary signal beneath the central Aleutians. The trench oblique measurements likely arise due to smaller-scale, localized features, discussed below. Trench parallel wedge splitting has been observed in several subduction zones world-wide [e.g. Wirth and Long, 2010; Long and Wirth, 2013], including in portions of the AASZ [Christensen and Abers, 2010; Long and Silver, 2008; Lynner, 2021; Yang et al., 2021]. Trench parallel splitting is likely tied to trench parallel anisotropy and along strike flow. As discussed above, the subducting Pacific slab terminates beneath Alaska allowing for trench parallel toroidal flow to emerge. Numerical models show that once established, return flow around a slab edge can produce trench parallel flow along much of a subduction zone [e.g. Capitanio and Faccenda, 2012; Jadamec and Billen, 2012]. We argue that the trench parallel splitting in the central Aleutians is tied to wide-spread trench parallel flow along the length of the subduction zone. This is consistent with previous studies that have argued for trench parallel flow in the AASZ [e.g. Christensen and Abers, 2010; Hanna and Long, 2012; Lynner, 2021; Yang et al., 2021].

The trench oblique fast directions in the central Aleutians are chiefly seen from events originating shallower than ~130km depth. These fast directions roughly parallel the motion of the Pacific plate (Fig. 2) and are likely related to entrainment of mantle material with the downgoing slab. As the slab subducts, it drags mantle wedge material down with it via 2D corner flow [e.g. Hall et al., 2000; Long et al., 2007]. Even in cases where 3D toroidal return flow dominates, there should be some entrainment of wedge material with the subducting slab [e.g. Faccenda and Capitanio, 2012; Long and Silver, 2008]. This creates plate motion aligned strains and associated anisotropy. Near the corner of the wedge where corner flow is most prevalent, the entrained layer may comprise the bulk of wedge anisotropy. Only once the trench parallel flow becomes established can trench parallel splitting be observed. The shallow events in our dataset may be sampling regions where the entrainment layer is still sufficiently strong to impact splitting and produce plate motion parallel fast directions. Once the wedge is thick enough to allow vigorous trench parallel flow, trench aligned splitting can emerge.

There may additionally be changes in olivine fabric type that complicate local-S splitting, leading to deviations from trench parallel orientations. Olivine B-type fabric can exist in the nose of mantle wedges and exhibits an orthogonal relationship between strain and fast direction to what is seen for the more common A-, C-, and E-type fabrics. The depth dependent splitting pattern between shallow and deep events could potentially be due to a transition to olivine B-type fabric. Deeper events create local-S waves that sample farther from the corner of the wedge and would therefore avoid sampling significant B-type fabrics, while shallow events are impacted by B-type fabric. This is unlikely the main cause of our splitting signal because the trench parallel and plate motion parallel fast directions are far from orthogonal, as would be predicted by a change in fabric type alone. It is more likely the plate motion aligned splitting is the result of slab entrainment, although changes in olivine fabric types cannot be ruled out.

4.3 Delay time variability along the AASZ

Throughout the AASZ, we do not see any significant variations in splitting with depth despite having event depths that span from 75km to over 200km. Delay times are largely consistent across the depth range with a few spurious large dt observations occurring at the shallowest depths, Fig. 3. Consistent delay times across event depths despite varying path lengths is observed in many local-S splitting studies [e.g. Wirth and Long, 2010]. This is potentially due to larger measurement scatter and errors associated with local-S splitting making discerning patterns in dt difficult. Karlowska et al. [2021], however, did observe a correlation between depth and average delay times beneath Alaska. While they also report significant scatter in individual delay times, the pattern persisted. This may suggest that a relationship between dt and path length is highly localized and examining larger regions masks this pattern in the AASZ. Alternatively, Karlowska et al. [2021] use a different frequency band for their shear wave splitting measurements than we use here. In Japan, frequency dependent local-S splitting was observed in the delay times [Wirth and Long, 2010]. If the AASZ also exhibits frequency dependent splitting, a relationship between dt and path length may only exist in the higher frequencies. The source of this discrepancy and potential frequency dependence warrants further study.

The central Aleutians also do not present a relationship between event depth and delay times but exhibit a lateral change in delay times along trench strike, Fig. 2. Westernmost measurements between 175ºE and 170ºW have an average delay time of ~1.4s while measurements between 170ºW and 160ºW have an average delay time of ~1.9s. There is, however, considerable scatter in dts recorded in each region. The primary difference between these adjacent regions is the obliquity of subduction, Fig 2. The plate motion in the westernmost region is more oblique to trench than in the region between 170ºW and 160ºW. This change in obliquity could account for the difference in dts by impacting the amount of strain necessary to align wedge anisotropy parallel to the trench. Where plate motion is more oblique to the trench, plate driven entrainment flow above the slab should be more closely aligned parallel to the trench simply due to geometry [e.g. Kneller and van Keken, 2008]. Wedge material would therefore require less deformation (and therefore strain) to rotate sufficiently to produce trench parallel anisotropy. Where plate motion is more orthogonal to the trench, a larger rotation in anisotropic direction is needed to create trench parallel splitting. Larger strains associated with greater rotations may be creating stronger anisotropy and consequently larger dts. We note, however, that the difference in subduction obliquity between both regions is ~25º. It is unclear if this is a sufficiently large change to create the deviation in splitting behavior that we observe.

Finally, there are a few very large dt (<2.5s) events in our local-S dataset. Such large delay times are difficult to attribute to simple olivine deformation in the mantle wedge due to the relatively short paths of the local-S waves. These large dt measurements are not restricted to any single region and tend to originate from shallower events. The shallower events can generate local-S phases with incidence angles of greater than ~15º. Incidence angles greater than 35º are rejected in shear wave splitting studies as shallow incidence angles can lead to conversions near the free surface that mimic splitting and may yield erroneous large dts [Wirth and Long, 2010]. The large dt events in this study, while having larger incidence angles, are all below the 35º cutoff, with some as low at ~16º. The large dts may be the result of dipping structures acting to increase the apparent incidence angle of the incoming S waves creating spurious conversions and large dts. The majority of larger incidence angle events, however, produce average delay time measurements. The cause of the large dt events is not immediately clear and warrants additional scrutiny.

Summary

We examine local-S shear wave splitting at broadband stations along the length of the Alaska-Aleutians subduction zone. Local-S splitting allows us to isolate anisotropy within the mantle wedge to examine patterns of mantle dynamics. We have dense measurement coverage in the central Aleutians and beneath Alaska. Beneath Alaska, we observe splitting measurements that rotate from trench orthogonal to trench parallel over a span of ~400km. This rotation in splitting direction is tied to toroidal flow around the edge of subducting Pacific plate. This style of toroidal flow has been suggested by numerical models of AASZ mantle dynamics. Our results lend great confidence to such models. In the central Aleutians, complex splitting orientations are observed, and they are mostly oriented parallel to the trench or the motion of the subducting plate. Splitting directions become more strongly trench parallel when only deeper events are considered suggesting trench parallel flow permeates the wedge. We propose that the patterns in splitting in Alaska and in the central Aleutians are both tied to dynamics associated with the edge of the subducting slab. Toroidal flow around the slab can account for the rotation in splitting directions beneath Alaska which then excites trench parallel flow throughout the wedge creating the trench parallel splitting in the Aleutians.

Figures

Figure 1. Station (Top) and event (Bottom) maps of our study region. (Top) Stations where recorded measurements were made are shown in red. Stations that were examined by yielded no measures are shown in white. (Bottom) Local events that met our criteria between 2019 and 2022 are shown. Event locations are colored by event depth.

Figure 2. (A) Local-S shear wave splitting measurement for our study region, (B) for the central Aleutians region, and (C) for the eastern Alaska region. Splitting results are plotted at the midpoint between the event and station. The orientations of the black bars denote fast splitting directions and the color of the circles show the measured delay times. Arrows show the motion of the subducting Pacific plate in the no-net-rotation reference frame [DeMets et al., 2010].

Figure 3. Plots of delay time (top) and trench relative fast directions (bottom) versus depth (left) and incidence angle (right) for the central Aleutians (blue) and Alaska (red) regions. Fast directions plotted relative to the strike of the trench such that a value of 0 is trench parallel. Individual measurement errors are shown.

Figure 4. Schematic cartoon of our preferred model. Toroidal flow around the edge of the subducting Pacific slab excites trench parallel flow along the length of the subduction zone. In the central Aleutians, while trench parallel flow dominates, plate motion entrainment is also present.

Acknowledgements

C. T-A. and E.P. were supported by the IRIS (now EarthScope Consortium) Research Experience for Undergraduates (NSF EAR-1852339). This work was funded by NSF OCE 1949210. Figures were made using the Generic Mapping Toolkit [Wessel et al., 2013]. We thank Xiaobo He, Ayoub Kaviani, and an anonymous reviewer for useful comments on this manuscript.

Data Availability

All seismic data used in this study is publicly available and was accessed through the Data Management Center of the EarthScope Consortium.

References

Bowman, J. R., & Ando, M. (1987). Shear-wave splitting in the upper-mantle wedge above the Tonga subduction zone. *Geophysical Journal International*, *88*(1), 25-41. 10.1111/j.1365-246X.1987.tb01367.x

Capitanio, F. A., & Faccenda, M. (2012). Complex mantle flow around heterogeneous subducting oceanic plates. *Earth and Planetary Science Letters*, *353*, 29-37. 10.1016/j.epsl.2012.07.042

Christensen, D. H., & Abers, G. A. (2010). Seismic anisotropy under central Alaska from SKS splitting observations. *Journal of Geophysical Research: Solid Earth*, *115*(B4). 10.1029/2009JB006712

Civello, S., & Margheriti, L. (2004). Toroidal mantle flow around the Calabrian slab (Italy) from SKS splitting. *Geophysical Research Letters*, *31*(10). 10.1029/2004GL019607

Crampin, S. & Peacock, S. (2008). A review of the current understanding of seismic shear-wave splitting in the Earth's crust and common fallacies in interpretation. *Wave Motion*, *45*(6), 675-722. 10.1016/j.wavemoti.2008.01.003

Davies, J., Sykes, L., House, L., & Jacob, K. (1981). Shumagin seismic gap, Alaska Peninsula: History of great earthquakes, tectonic setting, and evidence for high seismic potential. *Journal of Geophysical Research: Solid Earth*, *86*(B5), 3821-3855. 10.1029/jb086ib05p03821

Debayle, E., Dubuffet, F., & Durand, S. (2016). An automatically updated S-wave model of the upper mantle and the depth extent of azimuthal anisotropy. Geophysical Research Letters, 43, 674–682. 10.1002/2015GL067329

DeMets, C., Gordon, R. G., & Argus, D. F. (2010). Geologically current plate motions. *Geophysical journal international*, *181*(1), 1-80. 10.1111/j.1365-246X.2009.04491.x

Eberhart-Phillips, D., Christensen, D. H., Brocher, T. M., Hansen, R., Ruppert, N. A., Haeussler, P. J., & Abers, G. A. (2006). Imaging the transition from Aleutian subduction to Yakutat collision in central Alaska, with local earthquakes and active source data. *Journal of Geophysical Research: Solid Earth*, *111*(B11). 10.1029/2005JB004240

Faccenda, M., & Capitanio, F. A. (2012). Development of mantle seismic anisotropy during subduction-induced 3-D flow. *Geophysical Research Letters*, *39*(11). 10.1029/2012GL051988

Ferris, A., Abers, G. A., Christensen, D. H., & Veenstra, E. (2003). High resolution image of the subducted Pacific (?) plate beneath central Alaska, 50–150 km depth. *Earth and Planetary Science Letters*, *214*(3-4), 575-588. 10.1016/S0012-821X(03)00403-5

Fournier, T. J., & Freymueller, J. T. (2007). Transition from locked to creeping subduction in the Shumagin region, Alaska. *Geophysical Research Letters*, *34*(6). 10.1029/2006GL029073

Hall, C. E., Fischer, K. M., Parmentier, E. M., & Blackman, D. K. (2000). The influence of plate motions on three-dimensional back arc mantle flow and shear wave splitting. *Journal of Geophysical Research: Solid Earth*, *105*(B12), 28009-28033. 10.1029/2000JB900297

Hammond, J. O., Wookey, J., Kaneshima, S., Inoue, H., Yamashina, T., & Harjadi, P. (2010). Systematic variation in anisotropy beneath the mantle wedge in the Java–Sumatra subduction system from shear-wave splitting. *Physics of the Earth and Planetary Interiors*, *178*(3-4), 189-201. 10.1016/j.pepi.2009.10.003

Hanna, J., & Long, M. D. (2012). SKS splitting beneath Alaska: Regional variability and implications for subduction processes at a slab edge. *Tectonophysics*, *530*, 272-285. 10.1016/j.tecto.2012.01.003

Heuret, A., & Lallemand, S. (2005). Plate motions, slab dynamics and back-arc deformation. *Physics of the Earth and Planetary Interiors*, *149*(1-2), 31-51. 10.1016/j.pepi.2004.08.022

Honda, S. (2009). Numerical simulations of mantle flow around slab edges. *Earth and Planetary Science Letters*, *277*(1-2), 112-122. 10.1016/j.epsl.2008.10.003

IRIS Transportable Array. (2003). *USArray Transportable Array* [Data set]. International Federation of Digital Seismograph Networks. 10.7914/SN/TA

Jadamec, M. A., & Billen, M. I. (2010). Reconciling surface plate motions with rapid three-dimensional mantle flow around a slab edge. *Nature*, *465*(7296), 338-341. 10.1038/nature09053

Jadamec, M. A., & Billen, M. I. (2012). The role of rheology and slab shape on rapid mantle flow: Three-dimensional numerical models of the Alaska slab edge. *Journal of Geophysical Research: Solid Earth*, *117*(B2). 10.1029/2011JB008563

Jung, H., Katayama, I., Jiang, Z., Hiraga, T., & Karato, S. I. (2006). Effect of water and stress on the lattice-preferred orientation of olivine. *Tectonophysics*, *421*(1-2), 1-22. 10.1016/j.tecto.2006.02.011

Kaneshima, S. (1990). Origin of crustal anisotropy: Shear wave splitting studies in Japan. *Journal of Geophysical Research*, *95*(B7), 11121-11133. 10.1029/JB095iB07p11121

Karato, S. I., Jung, H., Katayama, I., & Skemer, P. (2008). Geodynamic significance of seismic anisotropy of the upper mantle: New insights from laboratory studies. *Annu. Rev. Earth Planet. Sci.*, *36*, 59-95. 10.1146/annurev.earth.36.031207.124120

Karlowska, E., Bastow, I. D., Rondenay, S., Martin-Short, R., & Allen, R. M. (2021). The development of seismic anisotropy below south-central Alaska: evidence from local earthquake shear wave splitting. *Geophysical Journal International*, *225*(1), 548-554. 10.1093/gji/ggaa603

Kincaid, C., & Griffiths, R. W. (2003). Laboratory models of the thermal evolution of the mantle during rollback subduction. *Nature*, *425*(6953), 58-62. 10.1038/nature01923

Király, Á., Capitanio, F. A., Funiciello, F., & Faccenna, C. (2017). Subduction induced mantle flow: Length-scales and orientation of the toroidal cell. *Earth and Planetary Science Letters*, *479*, 284-297. 10.1016/j.epsl.2017.09.017

Kneller, E. A., Long, M. D., & van Keken, P. E. (2008). Olivine fabric transitions and shear wave anisotropy in the Ryukyu subduction system. *Earth and Planetary Science Letters*, *268*(3-4), 268-282. 10.1016/j.epsl.2008.01.004

Kneller, E. A., & van Keken, P.E. (2008). Effect of three-dimensional slab geometry on deformation in the mantle wedge: Implications for shear wave anisotropy, *Geochemistry, Geophysics, and Geosystems*, 9, Q01003, 10.1029/2007GC001677.

Kong, F., Gao, S. S., Liu, K. H., Zhang, J., & Li, J. (2020). Seismic anisotropy and mantle flow in the Sumatra subduction zone constrained by shear wave splitting and receiver function analyses. Geochemistry, Geophysics, Geosystems, 21(2), e2019GC008766. 10.1029/2019GC008766

Lallemand, S., Heuret, A., & Boutelier, D. (2005). On the relationships between slab dip, back-arc stress, upper plate absolute motion, and crustal nature in subduction zones. *Geochemistry, Geophysics, Geosystems*, *6*(9). 10.1029/2005GC000917

Liu, K. H., Gao, S. S., Gao, Y., & Wu, J. (2008). Shear wave splitting and mantle flow associated with the deflected Pacific slab beneath northeast Asia. *Journal of Geophysical Research: Solid Earth*, *113*(B1). 10.1029/2007JB005178

Long, M. D., Hager, B. H., De Hoop, M. V., & Van Der Hilst, R. D. (2007). Two-dimensional modelling of subduction zone anisotropy with application to southwestern Japan. *Geophysical Journal International*, *170*(2), 839-856. 10.1111/j.1365-246X.2007.03464.x

Long, M. D., & Silver, P. G. (2008). The subduction zone flow field from seismic anisotropy: A global view. *science*, *319*(5861), 315-318. 10.1126/science.1150809

Long, M. D., & Silver, P. G. (2009). Mantle flow in subduction systems: The subslab flow field and implications for mantle dynamics. *Journal of Geophysical Research: Solid Earth*, *114*(B10). 10.1029/2008JB006200

Long, M. D., & van der Hilst, R. D. (2006). Shear wave splitting from local events beneath the Ryukyu arc: Trench-parallel anisotropy in the mantle wedge. *Physics of the Earth and Planetary Interiors*, *155*(3-4), 300-312. 10.1016/j.pepi.2006.01.003

Long, M. D., & Wirth, E. A. (2013). Mantle flow in subduction systems: The mantle wedge flow field and implications for wedge processes. *Journal of Geophysical Research: Solid Earth*, *118*(2), 583-606. 10.1002/jgrb.50063

Lynner, C. (2021). Anisotropy-revealed change in hydration along the Alaska subduction zone. *Geology*, *49*(9), 1122-1125. 10.1130/G48860.1

Lynner, C., Delph, J. R., Portner, D. E., Beck, S. L., Sandvol, E., & Özacar, A. A. (2022). Slab induced mantle upwelling beneath the Anatolian plateau. *Geophysical Research Letters*, *49*(11), e2021GL097451. 10.1029/2021GL097451

Lynner, C., & Long, M. D. (2014). Sub-slab anisotropy beneath the Sumatra and circum-Pacific subduction zones from source-side shear wave splitting observations. *Geochemistry, Geophysics, Geosystems*, *15*(6), 2262-2281. 10.1002/2014GC005239

Lynner, C., Long, M. D., Thissen, C. J., Paczkowski, K., & Montési, L. G. (2017). Evaluating geodynamic models for sub-slab anisotropy: Effects of olivine fabric type. *Geosphere*, *13*(2), 247-259. 10.1130/GES01395.1

Martin-Short, R., Allen, R., Bastow, I. D., Porritt, R. W., & Miller, M. S. (2018). Seismic imaging of the Alaska subduction zone: Implications for slab geometry and volcanism. *Geochemistry, Geophysics, Geosystems*, *19*(11), 4541-4560. 10.1029/2018GC007962

Maus, S., Barckhausen, U., Berkenbosch, H., Bournas, N., Brozena, J., et al. (2009). EMAG2: A 2–arc min resolution Earth Magnetic Anomaly Grid compiled from satellite, airborne, and marine magnetic measurements. *Geochemistry, Geophysics, Geosystems*, *10*(8). 10.1029/2009GC002471

McCormack, K., Wirth, E. A., & Long, M. D. (2013). B-type olivine fabric and mantle wedge serpentinization beneath the Ryukyu arc. *Geophysical Research Letters*, *40*(9), 1697-1702. 10.1002/grl.50369

McPherson, A. M., Christensen, D. H., Abers, G. A., & Tape, C. (2020). Shear wave splitting and mantle flow beneath Alaska. *Journal of Geophysical Research: Solid Earth*, *125*(4), e2019JB018329. 10.1029/2019JB018329

Perttu, A., Christensen, D., Abers, G., & Song, X. (2014). Insights into mantle structure and flow beneath Alaska based on a decade of observations of shear wave splitting. *Journal of Geophysical Research: Solid Earth*, *119*(11), 8366-8377. 10.1002/2014JB011359

Peyton, V., Levin, V., Park, J., Brandon, M., Lees, J., Gordeev, E., & Ozerov, A. (2001). Mantle flow at a slab edge: Seismic anisotropy in the Kamchatka region. *Geophysical Research Letters*, *28*(2), 379-382. 10.1029/2000GL012200

Piromallo, C., Becker, T. W., Funiciello, F., & Faccenna, C. (2006). Three-dimensional instantaneous mantle flow induced by subduction. *Geophysical Research Letters*, *33*(8). 10.1029/2005GL025390

Richards, C., Tape, C., Abers, G. A., & Ross, Z. E. (2021). Anisotropy variations in the Alaska subduction zone based on shear-wave splitting from intraslab earthquakes. *Geochemistry, Geophysics, Geosystems*, *22*(5), e2020GC009558. 10.1029/2020GC009558

Savage, M. K. (1999). Seismic anisotropy and mantle deformation: what have we learned from shear wave splitting?. *Reviews of Geophysics*, *37*(1), 65-106. 10.1029/98RG02075

Schellart, W. P., & Moresi, L. (2013). A new driving mechanism for backarc extension and backarc shortening through slab sinking induced toroidal and poloidal mantle flow: Results from dynamic subduction models with an overriding plate. *Journal of Geophysical Research: Solid Earth*, *118*(6), 3221-3248. 10.1002/jgrb.50173

Shillington, D. J., Bécel, A., Nedimović, M. R., Kuehn, H., Webb, S. C., Abers, G. A., et al. (2015). Link between plate fabric, hydration and subduction zone seismicity in Alaska. *Nature Geoscience*, *8*(12), 961-964. 10.1038/ngeo2586

Silver, P. G., & Chan, W. W. (1991). Shear wave splitting and subcontinental mantle deformation. *Journal of Geophysical Research: Solid Earth*, *96*(B10), 16429-16454. 10.1029/91jb00899

Song, W., Yu, Y., Gao, S. S., Liu, K. H., & Fu, Y. (2021). Seismic anisotropy and mantle deformation beneath the central Sunda plate. *Journal of Geophysical Research: Solid Earth*, *126*(3), e2020JB021259. 10.1029/2020JB021259

Stegman, D. R., Freeman, J., Schellart, W. P., Moresi, L., & May, D. (2006). Influence of trench width on subduction hinge retreat rates in 3-D models of slab rollback. *Geochemistry, Geophysics, Geosystems*, *7*(3). 10.1029/2005GC001056

Uchida, N., Nakajima, J., Wang, K., Takagi, R., Yoshida, K., Nakayama, T., et al. (2020). Stagnant forearc mantle wedge inferred from mapping of shear-wave anisotropy using S-net seafloor seismometers. Nature Communications, 11(1), 3549–8. 10.1038/s41467-020-19541-y

Venereau, C. M. A., Martin-Short, R., Bastow, I. D., Allen, R. M., & Kounoudis, R. (2019). The role of variable slab dip in driving mantle flow at the eastern edge of the Alaskan subduction margin: Insights from shear-wave splitting. *Geochemistry, Geophysics, Geosystems*, *20*(5), 2433-2448. 10.1029/2018GC008170

Wessel, P., Smith, W. H. F., Scharroo, R., Luis, J. & Wobbe, F. (2013) Generic mapping tools: improved version released. *Eos, Trans. Am. Geophys. Union* **94**, 409–410. 10.1002/2013eo450001

Wirth, E., & Long, M. D. (2010). Frequency-dependent shear wave splitting beneath the Japan and Izu-Bonin subduction zones. *Physics of the Earth and Planetary Interiors*, *181*(3-4), 141-154. 10.1016/j.pepi.2010.05.006

Wüstefeld, A., & Bokelmann, G. (2007). Null detection in shear-wave splitting measurements. *Bulletin of the Seismological Society of America*, *97*(4), 1204-1211. 10.1785/0120060190

Wüstefeld, A., Bokelmann, G., Zaroli, C., & Barruol, G. (2008). SplitLab: A shear-wave splitting environment in Matlab. *Computers & Geosciences*, *34*(5), 515-528. 10.1016/j.cageo.2007.08.002

Yang, X., Fischer, K. M., & Abers, G. A. (1995). Seismic anisotropy beneath the Shumagin Islands segment of the Aleutian-Alaska subduction zone. *Journal of Geophysical Research: Solid Earth*, *100*(B9), 18165-18177. 10.1029/95JB01425

Yang, Y., Gao, S. S., Liu, K. H., Kong, F., & Fu, X. (2021). Mantle flow in the vicinity of the eastern edge of the Pacific-Yakutat slab: Constraints from shear wave splitting analyses. *Journal of Geophysical Research: Solid Earth*, *126*(9), e2021JB022354. 10.1029/2021JB022354

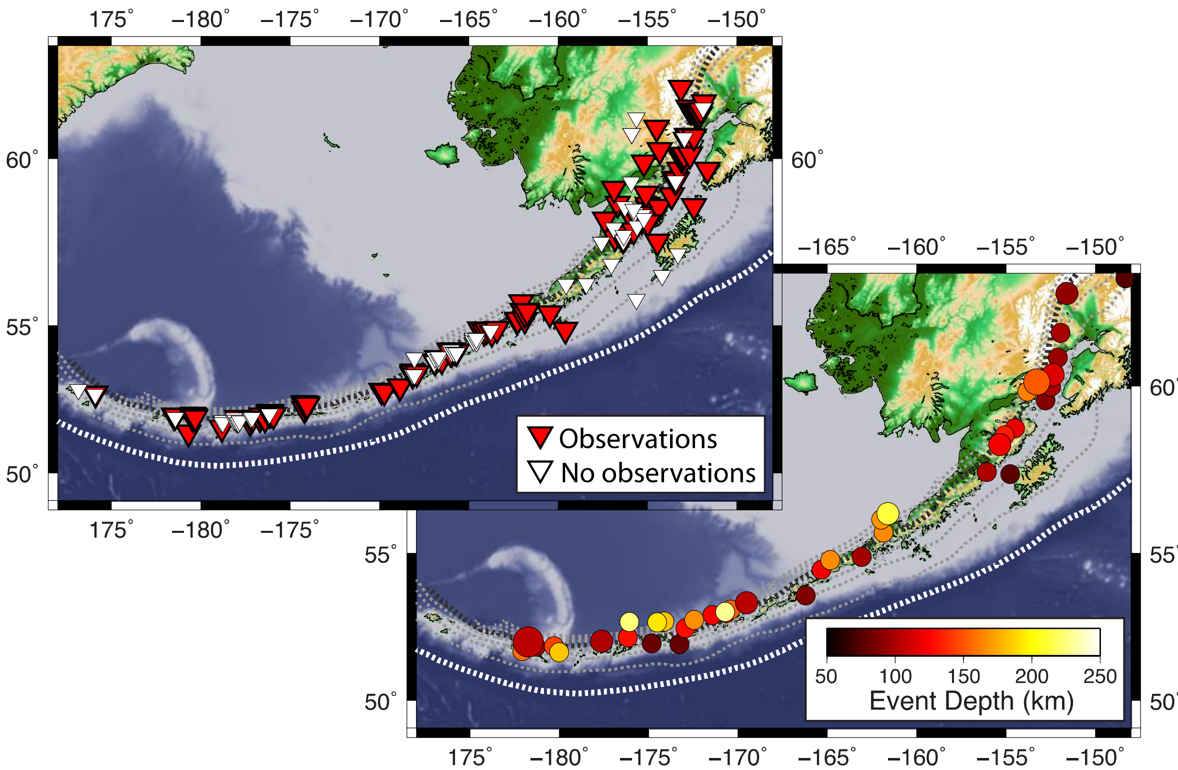

Figure 1. Station (Top) and event (Bottom) maps of our study region. (Top) Stations where recorded measurements were made are shown in red. Stations that were examined by yielded no measures are shown in white. (Bottom) Local events that met our criteria between 2019 and 2022 are shown. Event locations are colored by event depth.

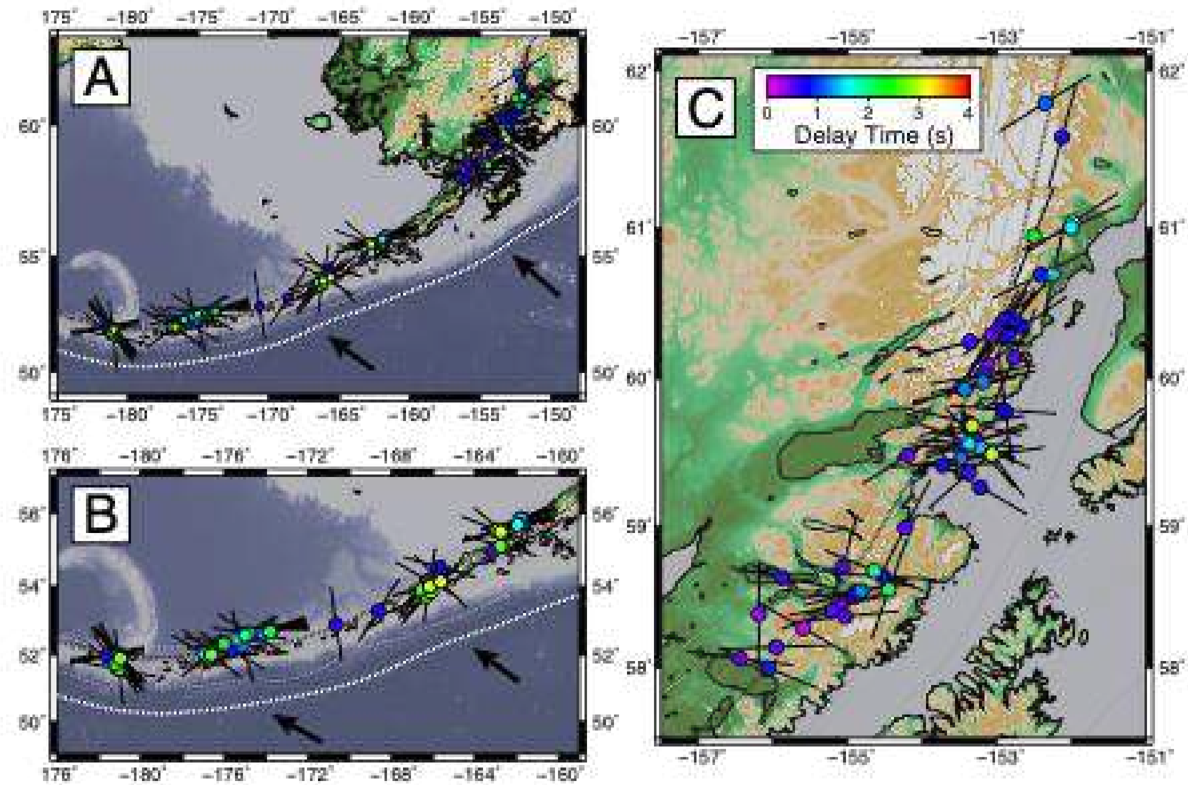

Figure 2. (A) Local-S shear wave splitting measurement for our study region, (B) for the central Aleutians region, and (C) for the eastern Alaska region. Splitting results are plotted at the midpoint between the event and station. The orientations of the black bars denote fast splitting directions and the color of the circles show the measured delay times. Arrows show the motion of the subducting Pacific plate in the no-net-rotation reference frame [DeMets et al., 2010].

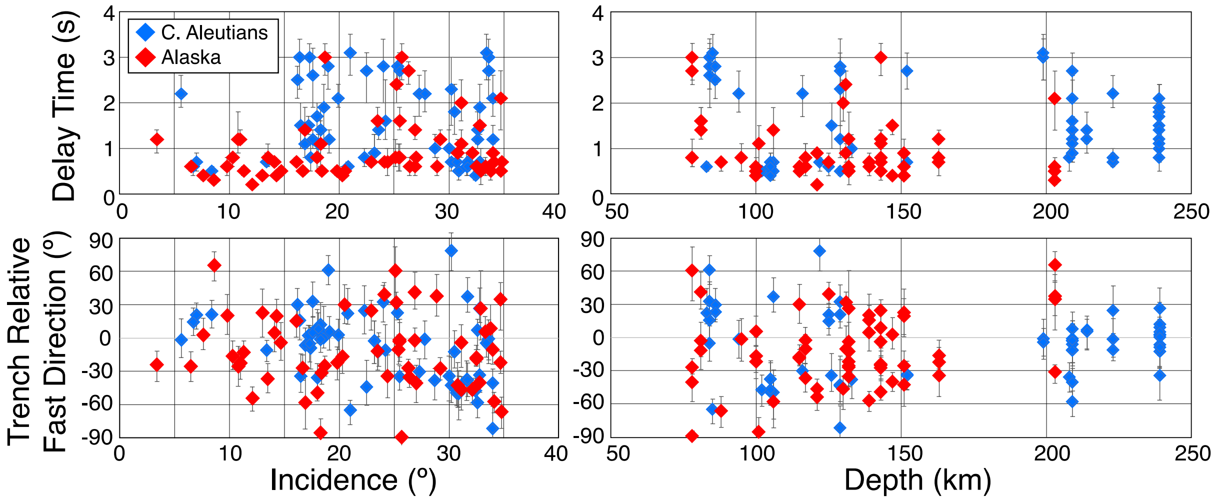

596

597 **Figure 3.** Plots of delay time (top) and trench relative fast directions (bottom) versus depth (left) and incidence angle (right) for the central Aleutians (blue) and Alaska (red) regions. Fast directions plotted relative to the strike of the trench such that a value of 0 is trench parallel. Individual error measurements are shown.

601

602

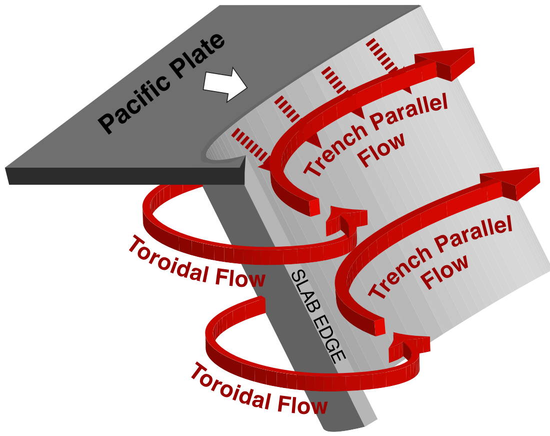

Figure 4. Schematic cartoon of our preferred model. Toroidal flow around the edge of the subducting Pacific slab excites trench parallel flow along the length of the subduction zone. In the central Aleutians, while trench parallel flow dominates, plate motion entrainment is also present.